BRAIN COMMUNICATIONS

Evaluation of [^{18}F]PI-2620, a second-generation selective tau tracer, for assessing four-repeat tauopathies

Toshiki Tezuka,[1] Keisuke Takahata,[2,3] Morinobu Seki,[1] Hajime Tabuchi,[2] Yuki Momota,[2] Mika Shiraiwa,[2] Natsumi Suzuki,[2] Ayaka Morimoto,[2] Tadaki Nakahara,[4] Yu Iwabuchi,[4] Eisuke Miura,[5] Yasuharu Yamamoto,[2] Yasunori Sano,[2] Kei Funaki,[2] Bun Yamagata,[2] Ryo Ueda,[6] Takahito Yoshizaki,[1] Kyoko Mashima,[7] Mamoru Shibata,[1,8] Munenori Oyama,[1] Kensuke Okada,[1] Masahito Kubota,[1] Hajime Okita,[5] Masaki Takao,[9,10] Masahiro Jinzaki,[4] Jin Nakahara,[1] Masaru Mimura[2] and Daisuke Ito[1]

Tau aggregates represent a key pathologic feature of Alzheimer's disease and other neurodegenerative diseases. Recently, PET probes have been developed for *in vivo* detection of tau accumulation; however, they are limited because of off-target binding and a reduced ability to detect tau in non-Alzheimer's disease tauopathies. The novel tau PET tracer, [^{18}F]PI-2620, has a high binding affinity and specificity for aggregated tau; therefore, it was hypothesized to have desirable properties for the visualization of tau accumulation in Alzheimer's disease and non-Alzheimer's disease tauopathies. To assess the ability of [^{18}F]PI-2620 to detect regional tau burden in non-Alzheimer's disease tauopathies compared with Alzheimer's disease, patients with progressive supranuclear palsy ($n = 3$), corticobasal syndrome ($n = 2$), corticobasal degeneration ($n = 1$) or Alzheimer's disease ($n = 8$), and healthy controls ($n = 7$) were recruited. All participants underwent MRI, amyloid β assessment and [^{18}F]PI-2620 PET (Image acquisition at 60–90 min post-injection). Cortical and subcortical tau accumulations were assessed by calculating standardized uptake value ratios using [^{18}F]PI-2620 PET. For pathologic validation, tau pathology was assessed using tau immunohistochemistry and compared with [^{18}F]PI-2620 retention in an autopsied case of corticobasal degeneration. In Alzheimer's disease, focal retention of [^{18}F]PI-2620 was evident in the temporal and parietal lobes, precuneus, and cingulate cortex. Standardized uptake value ratio analyses revealed that patients with non-Alzheimer's disease tauopathies had elevated [^{18}F]PI-2620 uptake only in the globus pallidus, as compared to patients with Alzheimer's disease, but not healthy controls. A head-to-head comparison of [^{18}F]PI-2620 and [^{18}F]PM-PBB3, another tau PET probe for possibly visualizing the four-repeat tau pathogenesis in non-Alzheimer's disease, revealed different retention patterns in one subject with progressive supranuclear palsy. Imaging-pathology correlation analysis of the autopsied patient with corticobasal degeneration revealed no significant correlation between [^{18}F]PI-2620 retention *in vivo*. High [^{18}F]PI-2620 uptake at 60–90 min post-injection in the globus pallidus may be a sign of neurodegeneration in four-repeat tauopathy, but not necessarily practical for diagnosis of non-Alzheimer's disease tauopathies. Collectively, this tracer is a promising tool to detect Alzheimer's disease-tau aggregation. However, late acquisition PET images of [^{18}F]PI-2620 may have limited utility for reliable detection of four-repeat tauopathy because of lack of correlation between post-mortem tau pathology and different retention pattern than the non-Alzheimer's disease-detectable tau radiotracer, [^{18}F]PM-PBB3. A recent study reported that [^{18}F]PI-2620 tracer kinetics curves in four-repeat tauopathies peak earlier (within 30 min) than Alzheimer's disease; therefore, further studies are needed to determine appropriate PET acquisition times that depend on the respective interest regions and diseases.

1 Department of Neurology, Keio University School of Medicine, Tokyo, Japan
2 Department of Neuropsychiatry, Keio University School of Medicine, Tokyo, Japan

Accepted June 28, 2021

3 Department of Functional Brain Imaging Research, National Institute of Radiological Sciences, National Institutes for Quantum and Radiological Science and Technology, Chiba, Japan
4 Department of Diagnostic Radiology, Keio University School of Medicine, Tokyo 160-8582, Japan
5 Department of Pathology, Keio University School of Medicine, Tokyo 160-8582, Japan
6 Office of Radiation Technology, Keio University Hospital, Tokyo 160-8582, Japan
7 Department of Neurology, Tokyo Saiseikai Central Hospital, Tokyo 108-0073, Japan
8 Department of Neurology, Tokyo Dental College Ichikawa General Hospital, Tokyo 272-8513, Japan
9 Department of Clinical Laboratory, National Center of Neurology and Psychiatry (NCNP), National Center Hospital, Tokyo 187-8551, Japan
10 Brain Bank, Mihara Memorial Hospital, Gunma 372-0006, Japan

Correspondence to: Daisuke Ito, MD, PhD,
Department of Neurology, Keio University School of Medicine,
35 Shinanomachi, Shinjuku-ku, Tokyo 160-8582, Japan,
E-mail: d-ito@jk9.so-net.ne.jp

Graphical Abstract

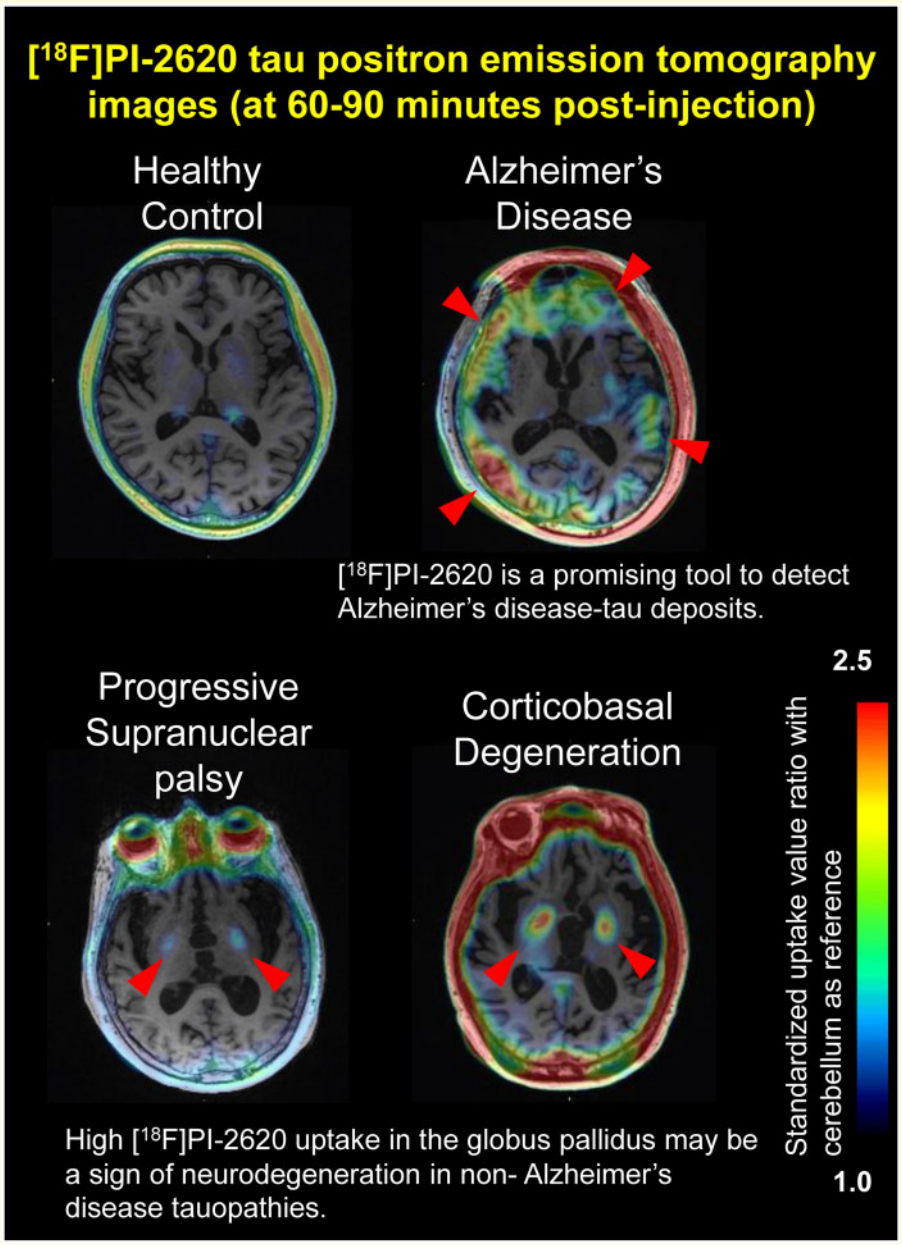

Keywords: Tau imaging; Alzheimer's disease; tauopathy; progressive supranuclear palsy; corticobasal degeneration

Abbreviations: 4R = four-repeat; ADAS-cog = Alzheimer's Disease Assessment Scale-cognitive subscale; AGD = argyrophilic grain dementia; CBD = corticobasal degeneration; CBS = corticobasal syndrome; DaTSCAN = dopamine transporter imaging; FBB = Florbetaben; FTLD = frontotemporal lobar degeneration; GM = grey matter; GMP = Good Manufacturing Practices; HCs = healthy controls; MMSE = Mini-Mental State Examination; PHFs = paired helical filaments; PSP = progressive supranuclear palsy; PSP-P = PSP-parkinsonism; PSPRS-J = PSP Rating Scale-Japan; PVC = partial-volume correction; ROIs = regions of interest; SUVRs = standardized uptake value ratios; UPDRS = Unified Parkinson's Disease Rating Scale; VOIs = volume of interests; WM = white matter

Introduction

PET ligands represent a potential innovative tool for the diagnostic accuracy and *in vivo* quantification of pathology in Alzheimer's disease and other tauopathies.[1,2] Several second-generation tau PET tracers, which have high selectivity and low affinity for 'off-target' factors, such as MAO-B or MAO-A, have been developed that enable high-contrast imaging of tau pathology in Alzheimer's disease, especially the three-repeat (3R) and four-repeat (4R) tau isoforms that aggregate into paired helical filaments (PHFs).[3] Additionally, tau PET is potentially useful for the *in vivo* assessment of non-Alzheimer's disease tauopathies, such as 4R tauopathy, progressive supranuclear palsy (PSP), corticobasal degeneration (CBD) and some variants of frontotemporal lobar degeneration (FTLD).[2,4]

With a pioneering tau tracer, [11C]PBB3, retention was observed in regions expected to harbour tau pathology in non-Alzheimer's disease tauopathies, such as PSP, corticobasal syndrome (CBS), and severe traumatic brain injury and chronic traumatic encephalopathy.[2,5,6] Some studies using [18F]AV1451 PET, which is the most widely studied tracer to date, have shown elevated retention in areas of frequent tau pathology in patients with PSP and CBS.[2,7,8] However, recent reports have failed to reveal any correlation between *in vivo* retention of radioligands and post-mortem tau measures in non-Alzheimer's disease tauopathies.[9,10] Similarly, a few studies have reported that the new tau tracer, [18F]PI-2620, binds to all types (3R, 4R and 3R/4R) of tau deposits *in vitro*,[11] but its reliability and usefulness *in vivo* as a biomarker in non-Alzheimer's disease tauopathies remains debatable.[11–17]

This study sought to evaluate tau PET imaging using [18F]PI-2620 in 4R tauopathies (patients with PSP, CBS and CBD). We characterized [18F]PI-2620 by comparison with [18F]PM-PBB3, another tau probe developed for tau fibrils in both Alzheimer's disease and non-Alzheimer's disease tauopathies, in the same PSP subject.[4,18,19] Finally, we correlated antemortem regional standardized uptake value ratios (SUVRs) of [18F]PI-2620 with post-mortem tau pathology, following the autopsy of a confirmed CBD case.

Materials and methods

Participants and clinical measurements

Patients with PSP ($n = 3$), CBS ($n = 2$), CBD ($n = 1$), and Alzheimer's disease ($n = 8$), and healthy controls (HCs) ($n = 7$) were recruited at Keio University Hospital from September 2018 to March 2020 (Table 1). We enrolled participants with ≥12 years of education. All participants underwent MRI scans. The diagnoses of Alzheimer's disease, PSP and CBS were made according to diagnostic criteria, as previously described.[20–22] Three PSP cases fulfilled the clinical criteria for probable PSP and their clinical predominance types were PSP with Richardson's syndrome in two cases and PSP–CBS in one case.[21] The CBS cases (#01, #17) had abnormal dopamine transporter imaging

Table 1 Participant characteristics and clinical test performance *in vivo* [18F]PI-2620 PET imaging

Disease	Non-Alzheimer's disease tauopathy ($n = 6$)	Alzheimer's disease ($n = 8$)	Healthy control ($n = 7$)
Sex (male/female)	2/4	4/4	4/3
Age, years (mean, SD)	71.8 ± 4.5	71.5 ± 8.7	71.1 ± 6.6
Education, years (mean, SD)	14.3 ± 2.0	13.5 ± 2.1	14.7 ± 3.3
MMSE (mean, SD)	13.7 ± 14.4	17.9 ± 5.3 #	28.4 ± 1.5
ADAS cog (mean, SD)	38.6 ± 34.4*	24.4 ± 8.4 # (1 N/A)	3.3 ± 1.2
Amyloid β PET (+/−)	2/3 (1 N/A)	8/0	0/7
UPDRS Part III (mean, SD)	64.5 ± 26.3	–	–
PSP Rating Scale (mean, SD)	66.8 ± 25.1	–	–

#Values reported reflect the mean ± standard deviation. *$P < 0.05$ (non-Alzheimer's disease tauopathy versus Healthy Control). $P < 0.05$ (Alzheimer's disease versus Healthy Control). Significant differences among groups for each value were assessed by a pairwise Wilcoxon test with a Bonferroni correction ($n = 3$).
ADAS, Alzheimer's Disease Assessment Scale; MMSE, Mini-Mental State Examination; N/A, not available; N/S, not significant; PSPRS, Progressive Supranuclear Palsy Rating Scale; SD, Standard Deviation; UPDRS, Unified Parkinson's Rating Scale.

(DaTSCAN) and asymmetric decreased cerebral blood flow in the frontoparietal areas in single-photon emission computed tomography. Phenotypically, they were classified as probable CBS and fulfilled clinical research criteria for probable sporadic CBD.[22] The enrolment criteria for HC and Alzheimer's disease participants were as follows. HC participants had Mini-Mental State Examination (MMSE) scores 24 and over; however, patients with Alzheimer's disease had MMSE scores ≤23. The Clinical Dementia Rating score for normal subjects was 0, while for patients with Alzheimer's disease 0.5 or 1. Delayed recall of one paragraph from the Logical Memory II subscale in the Wechsler Memory Scale–Revised was used to assess memory recall, with a cut-off score based on education: normal, ≥9 for 16 years of education, and ≥5 for 12–15 years of education. For patients with Alzheimer's disease, these scores were ≤8 for 16 years of education, and ≤4 for 12–15 years of education. For normal participants, the Geriatric Depression Scale score was <6. In addition, we performed the Alzheimer's disease Assessment Scale-cognitive component-Japanese version (ADAS-J cog)[23] and trail making test[24] in all participants; the Unified Parkinson's Disease Rating Scale (UPDRS) part III[25] in patients with PSP and CBD; and the PSP Rating Scale-Japan (PSPRS-J)[26] for patients with PSP.

Standard protocol approval, registration and patient consent

The study design and protocol were approved by the Ethics Committee for Human Research of the Keio University School of Medicine, and informed consent (#N20170237) was provided by all participants. The [^{18}F]PM-PBB3 study was approved by the Radiation Drug Safety Committee and National Institutes for Quantum and Radiological Science and Technology Certified Review Board of Japan. The study was registered with UMIN Clinical Trials Registry (UMIN-CTR; number 000032027 and 000030248).

[^{18}F]PI-2620 synthesis and PET acquisition

[^{18}F]PI-2620 was manufactured according to good manufacturing practices (GMP) at our hospital using an automated synthesizer (Synthera V2; IBA, Louvain-la-Neuve, Belgium). PET imaging was performed 60 min after intravenous administration of 185 MBq ± 10% [^{18}F]PI-2620 using a PET/CT system (Siemens Biograph mCT or Siemens Biograph mCT flow, Munich, Germany; these two pieces of equipment reflect the same level of competence because we did not use the 'flow-motion' setting for the brain scan). PET images were acquired for 30 min in a 3D list mode and serial image data (5-min, 10-min, 15-min and 20-min images) were reviewed to evaluate suitability for image interpretation (i.e. presence of head movement). For the visual [^{18}F]PI-2620 imaging, PET data were reconstructed by using the P-mod Neuro tool (PMOD Technologies, Switzerland) to produce cerebellar cortex references manually and to be anatomically fitted to the MR images. We also applied 'aparc + aseg volume' defined by FreeSurfer version 6.0 as regions of interest (ROIs). By using FSL, we calculated the conversion formula to anatomically fit MR T_1-weighted images to PET-CT images. The 'aparc + aseg volume' was placed on PET-CT images according to this conversion formula. The SUVR in each ROI was calculated using FSL. For the visual assessment of [^{18}F]PI-2620 imaging, the regional volumes of interest (VOIs) were set in the 8 regions identified in the National Institute of Neurological Disorders and Stroke and the Society neuropathological criteria for PSP, as having moderate to high tau burden (caudate nucleus, globus pallidus, putamen, thalamus, superiorfrontal gyrus, precentral gyrus, midbrain and pons). The brainstem ROIs were defined by using the Bayesian segmentation algorithm, based on a probabilistic atlas of the brainstem, available on FreeSurfer.[27] We calculated the SUVR to the cerebellar cortex and pericalcarine area as an index of [^{18}F]PI-2620 retention. Since the cerebellar cortex and pericalcarine area has far fewer tau deposits than the other cerebral cortex, even in non-Alzheimer's disease tauopathy,[28–33] it is considered an appropriate reference region for nonspecific binding. We performed a partial-volume correction (PVC) analysis using a template volume of interests based on individual masks derived from individual patient MR images using PMOD software [PVC using Template VOIs based on Individual Masks (pmod.com)]. We prepared anatomical MR images which were employed for a better individual adjustment for VOIs. The anatomical MRI of the patient was segmented and the grey matter (GM) and white matter (WM) masks were calculated. The MR image was normalized to the Montreal Neurological Institute MR template using the Brain Normalization method. The VOI template was transformed to the MR space using the inverse of the normalization transform. The transformed VOI template was intersected with the GM mask to obtain the GM VOIs in the MR space. The WM mask was converted into a WM VOI. The PET images were rigidly matched to the MR images. The GM and WM VOIs were transformed to the PET space using the inverse rigid transform. The contouring procedure was applied to get contour definitions of all VOIs. The Geometric Transfer Matrix PVC method was applied to the original PET series using this set of template-based VOIs.

[^{18}F] Florbetaben imaging

All subjects underwent [^{18}F] Florbetaben (FBB) PET scans, with the exception of one patient with CBD, whose amyloid-β deposition was assessed by autopsy. FBB was manufactured according to GMP in our hospital using an automated synthesizer (Synthera V2; IBA, Louvain-la-Neuve, Belgium). PET imaging was performed

as previously described.[34] The determination of amyloid β (Aβ) positivity or negativity was based on the assessment of tracer uptake in the GM of the four following brain regions: the lateral temporal lobes, frontal lobes, posterior cingulate cortex/precuneus and parietal lobes, in line with the NeuraCeq^{TM} guidelines.[35]

[18F]PM-PBB3 PET acquisition in PSP-CBS (#52)

One patient (#52) with PSP-CBS underwent PET scan with [18F]PM-PBB3 at the National Institute of Radiological Sciences. PET scan with [18F]PM-PBB3 was performed as described elsewhere.[4] Ninety minutes after an intravenous rapid bolus injection of [18F]PM-PBB3, three-dimensional images were acquired with a Biograph mCT flow system (Siemens Healthcare) for 20 min, providing 109 sections with an axial field of view of 16.2 cm. Images were reconstructed using a filtered back projection algorithm with a Hanning filter (4.0 mm full-width at half-maximum). [18F]PM-PBB3 had one injected dose of 184.4 MBq with a molar activity at the time of injection of 88.9 GBq/μmol. Regional SUVR values with the cerebellar cortex as a reference were calculated.

Quantitative assessment of tau burden

Subject #18 died two weeks after the [18F]PI-2620 PET scan due to aspiration pneumonia. For tissue-matched ROI analyses, 17 brain regions were selected for histological analysis based on expected PSP/CBD neuropathology. The brain was fixed by immersion in 20% formalin, cut in bihemispheric coronal slices and small regional samples, subsequently embedded in paraffin, and sectioned. Immunohistochemistry with AT8 (AT8 antibody, 1:10 000 dilution; DAKO), anti-4R tau (RD4), anti-3R tau (RD3, clone 8E6/C11), anti-α-synuclein (clone 42/α-Synuclein, 1:2000 dilution) and Aβ (clone 6F/3D, 1:200 dilution) antibodies was performed on 4-μm-thick tissue sections and modified Gallyas-Braak silver stain was applied to 6-μm–thick tissue sections. We used the pathological diagnostic criteria for CBD from Dickson's paper.[36] To assess tau burden, immunohistochemical images were colour-replaced with Photoshop and converted to 8-bit black-and-white images using ImageJ software (National Institutes of Health, Bethesda, MD, USA). A threshold to eliminate the background was determined using the cerebellar cortex. The percentage stained area was assessed using the Analyze %Area and Particle tool. When tau deposits presented in aggregates larger than approximately 2 µm, we defined these deposits as particles in ImageJ. The ROIs of SUVRs in PET/MRI image were manually determined to allow for alignment with the pathological samples by using MRIcroGL v1.2 (http://www.mccauslandcenter.sc.edu/mricrogl/). After repeated discussions with the neuropathologist, ROIs were created with cerebral cortex and nuclei used as landmarks so as to be correctly matched to the pathology specimen, ranging from about 4–17 mm × 4–18 mm with less than 900 µm thickness, which can be gauged as one voxel in MRIcroGL v1.2.

Statistical analysis

We used SPSS 26 (IBM Corp.) for statistical analyses. For group analysis of demographic data between groups, we used a Fisher's exact test (sex) and a pairwise Wilcoxon test with a Bonferroni correction ($n = 3$) (rest of the data). For analyses of [18F]PI-2620 SUVRs in ROIs, a pairwise Wilcoxon test with a Bonferroni correction ($n = 3$) was used. To assess the correlations between SUVRs and pathological values in autopsied and head-to-head patients, we used a Spearman test.

Data availability

Data are available from the corresponding author upon reasonable request.

Results

Participant characteristics and cognitive test performance

The demographic and clinical features of patients with non-Alzheimer's disease tauopathies (PSP, CBS and CBD), and those with Alzheimer's disease and HC are shown in Table 1. Their mean age at assessment was 71.8 ± 4.5 years (mean ± SD) in non-Alzheimer's disease tauopathies, 71.5 ± 8.7 years (mean ± SD) in Alzheimer's disease and 71.1 ± 6.6 years (mean ± SD) in HC. Patients with Alzheimer's disease were in a mild-to moderate clinical disease stage, as indicated by MMSE ($n = 8$, 17.9 ± 5.3), and ADAS-cog. ($n = 7$, 24.4 ± 8.4). All patients underwent [18F] FBB amyloid PET, with the exception of one patient with CBD (#18). [18F] FBB amyloid PET was positive for all Alzheimer's disease and two CBS patients, whereas all HC and all PSP patients were FBB-negative. In the autopsied patient with CBD (#18), there were no Aβ immunoreactive deposits in the cerebrum, cerebellum or brainstem.

Clinical course in the autopsied case with CBD (#18)

The patient was a 66-year-old female with a 5-year history of progressive limb rigidity, gait instability and levodopa resistance. Subsequently, she developed dysphagia, apathy/bradyphrenia, and limited vertical eye movements, and suffered from multiple falls, thereby identifying the clinical variant as PSP with Richardson's syndrome or

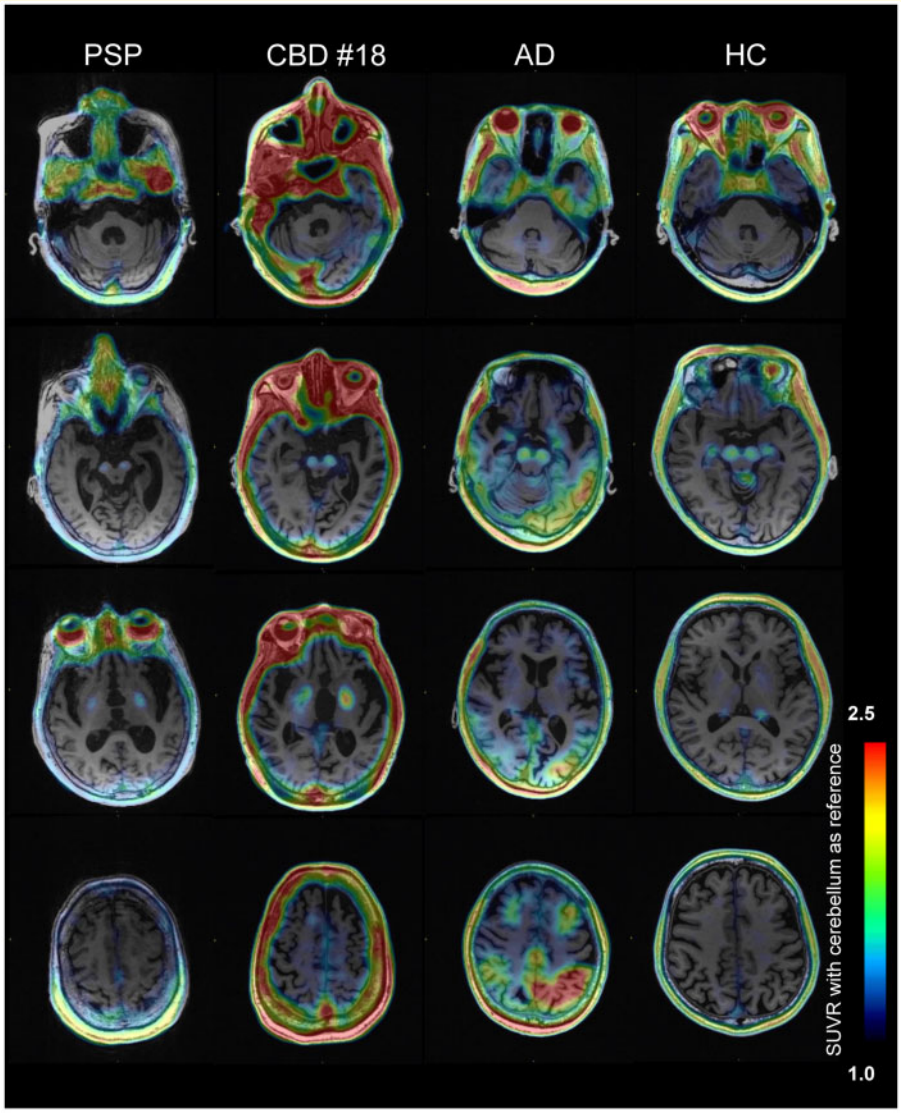

Figure 1 Representative images of [^{18}F]PI-2620 tau PET images. Individual tau PET images for patients with PSP, CBS, CBD, Alzheimer's disease and HC. All images are based on the same color scale (SUVR values ranging from 1 to 2.5). Cerebellar grey matter is used as the reference region for quantification. SUVRs, standardized uptake value ratios

predominant frontal presentation.[21] The patient also had a 4-year history of recurrent aspiration pneumonia.

At the time of PET scan with [^{18}F]PI-2620, she was severely demented and bedridden (PSP RS-J 90/100, UPDRS part III 92/132, MMSE 0). She died of pneumonia 14 days after a follow-up tau PET. A neuropathological examination showed numerous RD-4 immunoreactive neurons, threads, and astrocytic plaques in the cerebral cortex and basal ganglia, consistent with pathological signs of CBD.[36,37] There were no Aβ immunoreactive deposits in the cerebrum, cerebellum or brainstem. No α-synuclein immunoreactive deposits were present. There was no significant vascular pathology and particular other pathological findings. We diagnosed the subject (#18) as having CBD.

Clinical course of PSP-CBS case (#52)

The patient was a 74-year old male, with a 7-year history of right dominant tremor, limb rigidity, bradykinesia and progressive gait disturbance. No specific finding was detected on a brain MRI scan. DaTSCAN showed reduced uptake in striatum, predominantly in the left side. ^{123}I-meta-iodobenzylguanidine (MIBG) myocardial scintigraphy demonstrated normal myocardial uptake. His symptoms showed gradual progression, with levodopa treatment-resistance. He subsequently developed evident postural instability and ideomotor apraxia in his right hand. Although ocular motor dysfunction has not been shown so far, he is suspected to be PSP-CBS (PSPRS-J

33/100, UPDRS part III 52/132, MMSE 30).[21] After [18F]PM-PBB3 PET, [18F]PI-2620-PET imaging has done 8 months later to compare the retention of two tau radiotracers.

In vivo [18F]PI-2620-PET imaging

Figure 1 represents a selection of [18F]PI-2620 SUVR images overlaid on native-space MRI. [18F]PI-2620 scans in HC showed strong elevated retention in regions outside the brain, including skin/scalp, retina, nasal cavity and sinus veins (Fig. 1; Supplementary Fig. 1A and B). Significant, but variable, tracer retention was also observed as a high signal in the substantia nigra, and as a moderate signal in the choroid plexus and basal ganglia. This pattern indicated off-target binding in vessels, (neuro)melanin, iron-associated regions, and calcifications, similar to previous reports with the [18F]AV-1451 tau tracer.[37]

In patients with Alzheimer's disease, [18F]PI-2620 retention was evident in the temporal lobe, parietal lobe and cingulate cortex, consistent with the neuropathology of Alzheimer's disease. Notably, PET scans of the majority of clinical phenotypes of 4R tauopathies (PSP, CBS and CBD) revealed elevated retention in the globus pallidus, possibly reflecting neurodegeneration. Considering partial volume effects due to atrophy, PVC views also show similar findings (Supplementary Fig. 2). However, it could be challenging to visually identify 4R tauopathies because of varying levels of globus pallidus retention in HC and Alzheimer's disease (Fig. 1, Supplementary Fig. 1).

Differences in [18F]PI-2620 uptake patterns in patients with Alzheimer's disease, and non-Alzheimer's disease tauopathies

We assessed [18F]PI-2620 uptake in 8 subsets of ROIs for patients with 4R tauopathies, Alzheimer's disease and HC (Fig. 2). As shown in Fig. 2, patients with PSP, CBS and CBD had significant increases in [18F]PI-2620 uptake in the globus pallidus when compared to Alzheimer's disease patients ($P = 0.0024$); however, uptake was also apparent in HC, possibly due to high off-target binding in this region in HC. Unexpectedly, patients with PSP, CBS and CBD did not show increased [18F]PI-2620 uptake in the pons, superior frontal, and precentral cortices or caudate nucleus where 4R-tau depositions were expected. Using the pericalcarine area reference, which is known for its low tau burden in non-Alzheimer's disease,[32,33] instead of a cerebellar cortex reference for generating SUVR values resulted in similar findings (Supplementary Fig. 3). Although the reason is unknown, the caudate nucleus of Alzheimer's disease patients curiously shows significant low retention compared to HC, only when using the pericalcarine area reference ($P = 0.0092$) (Supplementary Fig. 3). Collectively, we concluded that the [18F]PI-2620 SUVR values in the globus pallidus could be helpful for identified patients with PSP and CBS; however, retention does not reliably reflect 4R-tau distribution.

Correlation of [18F]PI-2620 retention with neuropathology in CBD

We next compared *in vivo* [18F]PI-2620 retention to histopathological analysis results to gauge its ability to accurately reflect the abundance of tau depositions. In subject #18, the quantification of tau burden in AT8-immunostained sections revealed robust loads of tau lesions in multiple ROIs (Fig. 3). As shown in Fig. 3, in substantia nigra and globus pallidus, both tracer retention and tau burden are high. However, no significant correlation on all regions could be detected between [18F]PI-2620 PET retention and tau burden (Tau stage, %Area and particles) in matching ROIs. Notably, SUVRs were rather low in the middle frontal gyrus, hippocampus, and midbrain tectum, while high tau accumulations were detected. Taken together, these findings showed that the [18F]PI-2620 PET signal did not accurately reflect tau pathology.

Head-to-head comparison of [18F]PI-2620 and [18F]PM-PBB3 in patients with PSP-CBS (#52)

[11C]PBB3 is reported to be selective for diverse tau fibril strains compared to [11C]AV-1451 and could possibly identify the regional pattern of tau pathology in the CBS/PSP spectrum.[2,38] Additionally, recent studies have reported that a novel PBB3 derivative, [18F]PM-PBB3, could image three- and four-repeat tau lesions in non-Alzheimer's disease tauopathies, including biopsied and autopsy-confirmed subjects.[4] To further characterize [18F]PM-PBB3, we compared the retention of both radiotracers in the same subject (#52) with PSP-CBS. In [18F]PM-PBB3 scanning, retention was evident in the midbrain (substantia nigra and red nucleus), subthalamic nucleus, thalamus, globus pallidus and precentral gyrus, consistent with the expected neuropathology of PSP (Fig. 4A and Supplementary Fig. 4). [18F]PM-PBB3 retention was left dominant in each ROI, consistent of the right dominant parkinsonism and apraxia in this subject and that DaTSCAN showed reduced uptake especially in the left striatum. Also, the relatively evident uptake in the precentral gyrus reflected his subsequent apraxia as PSP-CBS.

In addition to the absence of any significant correlation between both tracer SUVRs, different accumulation patterns were observed in multiple brain regions, including the precentral gyrus, red nucleus, subthalamic nucleus and thalamus (Fig. 4B). This finding revealed the differential *in vivo* binding properties of [18F]PI-2620 and [18F]PM-PBB3 in non-Alzheimer's disease tauopathies.

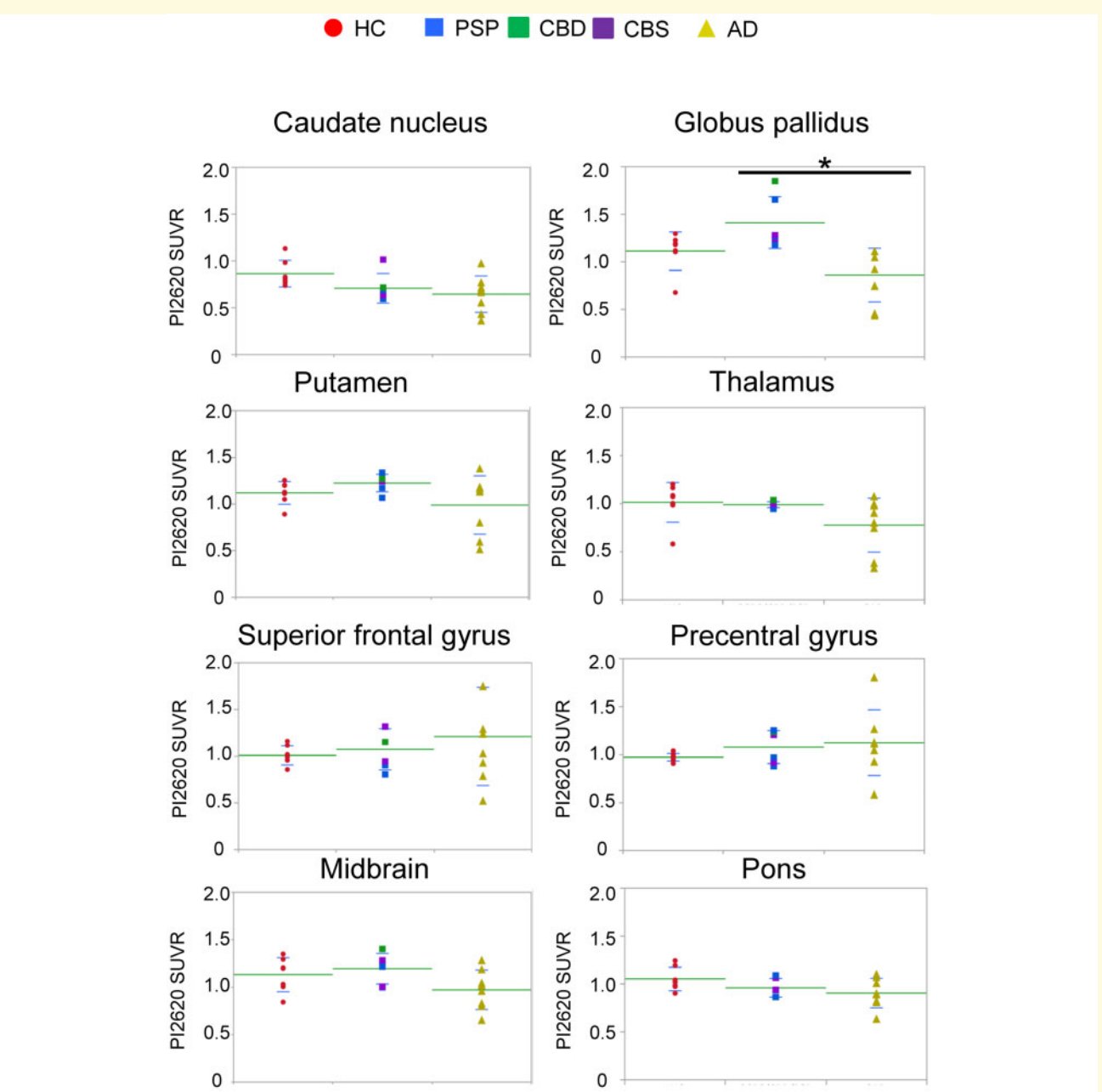

Figure 2 [^{18}F]PI-2620 standardized uptake value ratios in regions of interest. Graphs showing the distribution of [^{18}F]PI-2620 SUVRs in eight ROIs for patients with HC (red), PSP (blue) + CBD (green) + CBS (purple), and Alzheimer's disease (yellow). Dots represent individual subject SUVRs for each ROI. Significant pairwise Wilcoxon tests with a Bonferroni correction between diagnostic groups ($n = 3$) are indicated at the top: *$P < 0.05$

Discussion

In this study, we assessed the novel tau PET radiotracer, [^{18}F]PI-2620, in patients with Alzheimer's disease and 4R tauopathies (PSP, CBS and CBD), and demonstrated the first pathologic validation of tau positivity in autopsied CBD, and a head-to-head comparison with another tau PET probe for visualizing 4R-tau pathogenesis in non-Alzheimer's disease, [^{18}F]PM-PBB3. Further, SUVR analyses revealed that, compared with Alzheimer's disease patients, patients with 4R tauopathies showed elevated [^{18}F]PI-2620 uptake in the globus pallidus. However, the diagnostic potential for distinguishing 4R tauopathies is limited due to tracer retention in globus pallidus in HC. We also did not find a correlation between post-mortem tau pathology and *in vivo* region-matched [^{18}F]PI-2620 retention in a patient with CBD. Indeed, the autopsy findings were more likely to reflect the tau burden at the time of PET because of the short interval between the tau PET and the subsequent autopsy (two weeks).

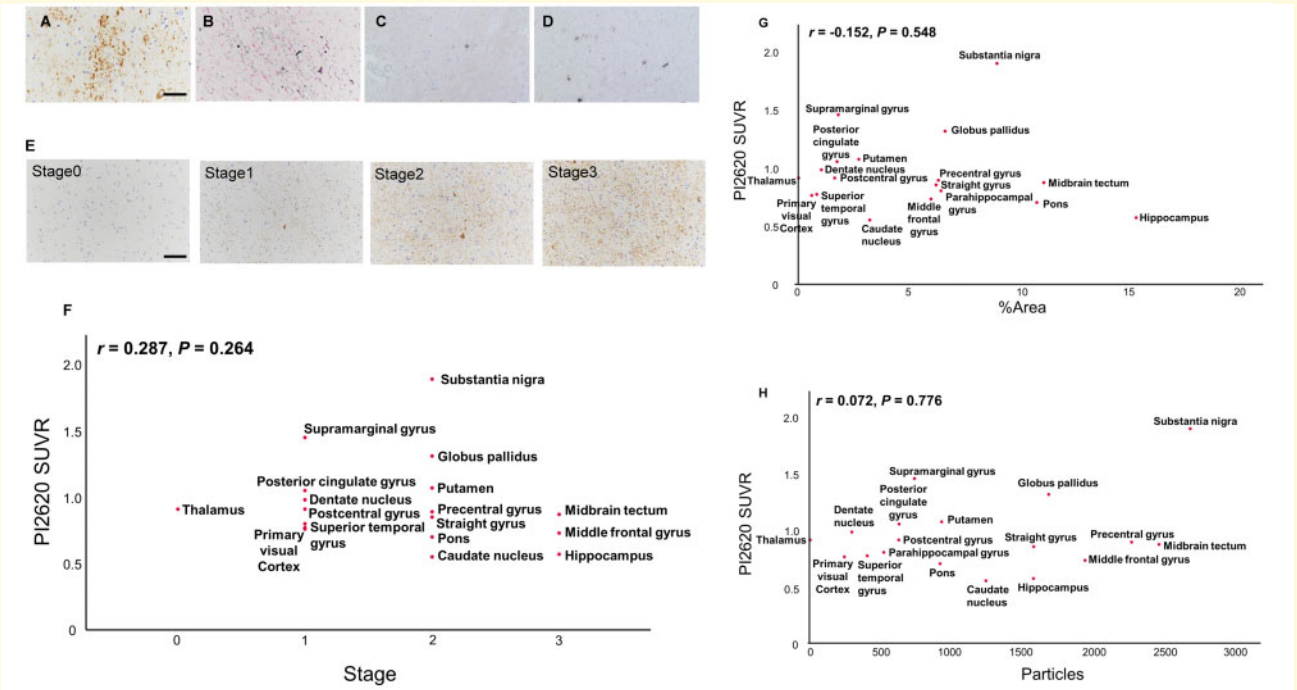

Figure 3 Neuropathological assessment of tau pathology and correlations with [18F]PI-2620 uptake in autopsied CBD. (**A–D**) Immunohistochemistry [AT8 (A), RD3 (C) and RD4 (D)] and Gallyas silver staining (B) in case #18. Scale bars indicate 50 μm (A and B) and 100 μm (C and D). (A) Caudate nucleus, (B) Straight gyrus, (C and D) Substantia nigra. Representative astrocytic plaque was detected in caudate nucleus (A). (**E**) Staging of AT8 staining [Stage 0 (Occipital lobe): absent, Stage 1 (Occipital lobe): sparse, Stage 2 (Precentral gyrus): moderate, Stage 3 (Superior colliculus): numerous] Scale bars indicate 100 μm. (**F–H**) Correlation analysis between *in vivo* [18F]PI-2620 SUVR and tau staging (F), %area (G) or particles (H) of AT8 staining in matching ROIs. *P*-values for Spearman correlation test.

Collectively, high [18F]PI-2620 uptake in the globus pallidus may be a sign of neurodegeneration in four-repeat (4R) tauopathies, but not necessarily a practical for diagnosis of dementia. We consider that this tracer may have limited utility for the reliable detection of 4R-tau pathologies.

While preparing this manuscript, Brendel et al. reported [18F]PI-2620 PET imaging in a patient cohort with clinically diagnosed PSP and Aβ-positive/negative CBS.[14,39] They evaluated distribution volume ratio images in a full dynamic setting (0–60 min post-injection) and revealed elevated [18F]PI-2620 binding in patients with PSP only in the globus pallidus and subthalamic nucleus, but not in other regions, such as the prefrontal cortex and dorsal midbrain. Notably, they also observed no correlation between [18F]PI-2620 binding and clinical severity or disease duration in any target regions. These findings strongly support our result that the [18F]PI-2620 PET signal did not accurately reflect 4R tau pathology.

Similar findings were reported using other tau tracers, such as [18F]AV1451, [18F]RO948 and [18F]THK5351.[7,8,40–42] Retention of these radiotracers was observed in the basal ganglia of patients with PSP; however, *in vivo* retention did not correlate with post-mortem tau accumulation,[10,43] supporting the present [18F]PI-2620 findings (Figs 2 and 3).

In addition, comparing [18F]PI-2620 retention in the same subject with a well-studied radiotracer, [18F]PM-PBB3, was important to further define the properties of our novel tracer. PBB3 derivatives have unique structures, characterizing their distinct tau affinities. [18F]PM-PBB3 is considered a possible PET tracer for detection of tau fibrils in 4R tauopathies.[4] In our subject with PSP-CBS, [18F]PM-PBB3 retention was evident in the frontal, parietal lobe, subthalamic nucleus, midbrain and pons, consistent with the expected PSP neuropathology. However, [18F]PI-2620 distribution was different, especially in the frontal and parietal cortex, related to CBS symptoms (Fig. 4A and Supplementary Fig. 4). Although further pathological and neuroimaging studies are needed to validate its utility for detection of non-Alzheimer's disease tau deposition, the present findings strongly propose that [18F]PI-2620 has a distinct capacity for tau deposition in non-Alzheimer's disease tauopathies compared to PBB3 derivatives.

Our study has several limitations. First, pathological results showed that [18F]PI-2620 retention did not reflect deposition of twisted ribbon filaments of 4R-tau in one autopsied CBD brain, but not other tauopathies. Non-Alzheimer's disease tau aggregates are varied structurally and accumulate in different cell types.[44,45] Importantly, Brendel et al. showed that post-mortem autoradiographies

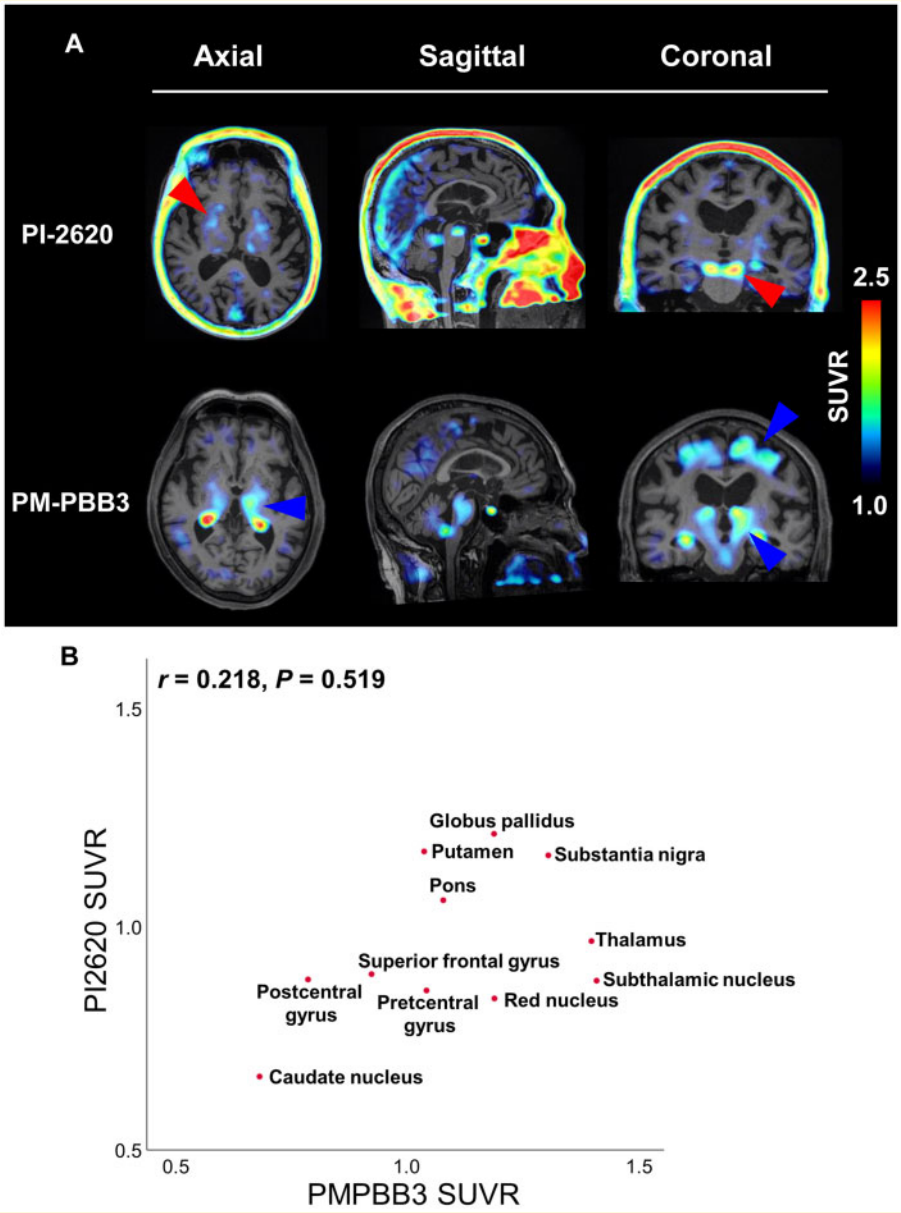

Figure 4 Head-to-head comparison of [^{18}F]PI-2620 and [^{18}F]PM-PBB3 in patients with PSP-CBS (#52). (**A**) [^{18}F]PI-2620 and [^{18}F]PM-PBB3 imaging in subject #52 representative of range of tracer binding. Transaxial and coronal [^{18}F]PI-2620 images adjacent to same-slice [^{18}F]PM-PBB3 images are shown. Red arrowheads indicate positive retention of both [^{18}F]PI-2620 and [^{18}F]PM-PBB3 (globus pallidus and substantia nigra). Blue arrowheads indicate positive [^{18}F]PM-PBB3 retention, but weak [^{18}F]PI-2620 (thalamus, frontal gyrus and subthalamic nucleus). (**B**) Plot of SUVR for [^{18}F]PI-2620 and [^{18}F]PM-PBB3 in matching ROIs. *P*-values for Spearman correlation test.

of the basal ganglia and frontal cortex slices clearly showed blockable [^{18}F]PI-2620 binding in patients with PSP, consistent with tau-immunohistochemistry.[14] Therefore, we cannot deny the possibility that [^{18}F]PI-2620 has substantial affinity to other forms of 4R-tau, such as straight filaments in patients with PSP, and straight filaments or tubules in argyrophilic grain dementia (AGD). In addition, we do not have any data at this point for [^{18}F]PI-2620 uptake in 3R tauopathies, such as Pick's disease. Future imaging-pathology dual studies are required to determine the association between tau burden in PSP, AGD, and Pick's disease post-mortem and *in vivo* [^{18}F]PI-2620 retention.

Second, Brendel et al. observed time–activity ratio curves are rapidly decreasing in the basal ganglia of PSP cases until 60 min after a peak within the first 30 min.[14,39] They recommend 30–60 min post-injection for PET acquisition of PSP and CBD. In contrast, illustrative time–activity curves and SUVRs plateau at 60–90 min in Alzheimer's disease.[46] Notably, time-SUVRs-curves in Brendel et al.'s study also show other expected tau-deposit regions in PSP,

such as the substantia nigra, the dorsal midbrain and dentate nucleus, revealing different tracer kinetics from those of the basal ganglia.[14] To practically establish evidence of the utility of tau PET for memory clinics and general medical care, we acquired the [18F]PI-2620 PET images at 60–90 min post-injection focussing on Alzheimer's disease in this study. On the other hand, recent studies reveal that early time frames for PI-2620 PET in 4R tauopathies is worthwhile.[14,39] Therefore, further studies need to evaluate two-time frames of [18F]PI-2620 imaging (early frame; 30–60 and late frame; 60–90 min) and/or determine appropriate PET acquisition times that depend on the respective interest regions and diseases.

Third, the retention target of [18F]PI-2620 in the globus pallidus in 4R tauopathies remains unknown. Off-target binding in the basal ganglia is commonly observed in [18F]AV-1451 PET studies of the elderly. Recent studies have shown that [18F]AV-1451 exhibits off-target binding to melanin, calcifications and iron accumulation sites.[37,47–49] Furthermore, the basal ganglia express high aminergic projections and neuroreceptors, and shows progressive neurodegeneration and astro-microgliosis in non-Alzheimer's disease tauopathy. Therefore, *in vitro* binding assays and autoradiography using fresh-frozen brain samples are required to accurately interpret *in vivo* [18F]PI-2620 PET positivity in 4R tauopathy.

Fourth, multiple diseases exhibit CBS phenotypes, and CBS's pathological background is broad. Two CBS cases (#01 and #17) showing cortical retention of [18F]PI-2620 PET in our study (Supplementary Fig. 5), were FBB positive, indicating overlapping Aβ pathology. A review of clinicopathological series reported that the most common pathologic substrates for clinical CBS are CBD (46.7%), Alzheimer's disease (16.7%), PSP (16.1%), FTLD with TDP-43 pathology (6.7%) and Pick's disease (3.9%).[50] Aβ pathology is found to frequently overlap with CBD.[51] However, given that both show typical CBS symptoms, DaTSCAN abnormalities, and higher [18F]PI-2620 retention in the globus pallidus, we propose that both pathological diagnoses are CBS–CBD concomitant with Alzheimer's disease pathology and high uptake in globus pallidus has diagnostic value to distinguish between typical Alzheimer's disease and CBS-CBD concomitant with Alzheimer's disease pathology.

Based on the current pathology-imaging study showing limited [18F]PI-2620 cortical uptake in autopsy-confirmed CBD (Fig. 3), it is likely that increased [18F]PI-2620 cortical retention in both CBS cases mostly reflect the PHF burden of Alzheimer's disease pathology. Recently, Palleis reported Aβ-positive CBS patients showed regional [18F]PI-2620 retentions in pre- and postcentral gyri, which were spared in Aβ-positive typical Alzheimer's disease patients with amnestic syndromes,[14,39] which may support our results that Aβ-positive CBS cases, in particular #17, showed [18F]PI-2620 retentions in left postcentral gyrus (Supplementary Fig. 5), whereas Alzheimer's disease patients curiously showed decreased [18F]PI-2620 uptake in the globus pallidus (Fig. 2 and Supplementary Fig. 3). Further pathology-imaging studies are needed to interpret [18F]PI-2620 retentions in Aβ-positive CBS.

Fifth, our study shows only one head-to-head analysis in a PSP patient. [18F]PMPBB3 is considered a possible PET tracer for the detection of tau fibrils in 4R tauopathies based on a single study with a limited sample size.[4,18,19] Another study suggests that the limited specificity of the original compound, [11C]PBB3, for tau and a potential binding affinity of the tracer for the more abundant Aβ in the Alzheimer's disease brain.[52] Possibility of unknown off-target bindings of [18F]PM-PBB3 need to be investigated with thorough further ante-/post-mortem investigations. With regard to the eventual conclusion of a possible PET tracer for diagnosis and differentiation of non-Alzheimer's disease tauopathies, further clinicopathological assessments will be required.

Collectively, this study laid evidence that [18F]PI-2620 PET uptake at a late time frame in the globus pallidus may be associated with its degeneration in non-Alzheimer's disease 4R tauopathies. We also found no correlation between *in vivo* retention at a late time frame and post-mortem tau accumulation in autopsy-confirmed CBD. Although further large-scale studies and detailed assessments of scan imaging and procedures are required to exploit its full potential, this tau tracer is a promising PET radioligand for *in vivo* imaging of tau aggregates in Alzheimer's disease, but of limited utility for the reliable detection of 4R-tau pathology at 60–90 min post-injection. We propose that tau tracers should be used differently depending on the tau fibrils of Alzheimer's disease or non-Alzheimer's disease tauopathies.

Supplementary material

Supplementary material is available at *Brain Communications* online.

Acknowledgements

The authors would like to thank Mr Kiyotaka Nakajima, Mr Kouki Oumi, Mr Yosinori Taniguchi, Mr Kazuya Minamishima, Mr Yoshiki Oowaki, and the staff of the Division of Nuclear Medicine and the Department of Radiology for their help in PET examinations and image processing. We thank the following individuals for analysis of tau imaging: Dr Kenji Tagai, Dr Hitoshi Shimada and Dr Makoto Higuchi at Department of Functional Brain Imaging Research, National Institute of Radiological Sciences, National Institutes for Quantum and Radiological Science and Technology, Chiba, Japan. We are also grateful to the following individuals for clinical assistance and comments: Dr Toshie Kitao and Dr Ryo Shikimoto, Department of Neuropsychiatry/Memory Center, Keio University School of Medicine, Japan. We thank Mitsutoshi Tano and Kiyora

Nakajima and Satoshi Kusakari for technical support in neuropathological analysis.

Funding

This research was supported by Japan Agency for Medical Research and Development under Grant Number JP17pc0101006 and supported in part by Japan Society for the Promotion of Science KAKENHI Grant Number 16H06277.

Competing interests

All authors declare no competing interests.

References

1. Klunk WE, Engler H, Nordberg A, et al. Imaging brain amyloid in Alzheimer's disease with Pittsburgh Compound-B. Ann Neurol. 2004;55(3):306–319.
2. Maruyama M, Shimada H, Suhara T, et al. Imaging of tau pathology in a tauopathy mouse model and in Alzheimer patients compared to normal controls. Neuron. 2013;79(6):1094–1108.
3. Lohith TG, Bennacef I, Vandenberghe R, et al. Brain imaging of Alzheimer dementia patients and elderly controls with (18)F-MK-6240, a PET tracer targeting neurofibrillary tangles. J Nucl Med. 2019;60(1):107–114.
4. Tagai K, Ono M, Kubota M, et al. High-contrast in vivo imaging of tau pathologies in Alzheimer's and non-Alzheimer's disease tauopathies. Neuron. 2021;109(1):42–58 e8.
5. Takahata K, Kimura Y, Sahara N, et al. PET-detectable tau pathology correlates with long-term neuropsychiatric outcomes in patients with traumatic brain injury. Brain. 2019;142(10):3265–3279.
6. Endo H, Shimada H, Sahara N, et al. In vivo binding of a tau imaging probe, [(11) C]PBB3, in patients with progressive supranuclear palsy. Mov Disord. 2019;34(5):744–754.
7. Schonhaut DR, McMillan CT, Spina S, et al. (18) F-flortaucipir tau positron emission tomography distinguishes established progressive supranuclear palsy from controls and Parkinson disease: A multicenter study. Ann Neurol. 2017;82(4):622–634.
8. Smith R, Scholl M, Widner H, et al. In vivo retention of (18)F-AV-1451 in corticobasal syndrome. Neurology. 2017;89(8):845–853.
9. Passamonti L, Vazquez Rodriguez P, Hong YT, et al. 18F-AV-1451 positron emission tomography in Alzheimer's disease and progressive supranuclear palsy. Brain. 2017;140(3):781–791.
10. Marquie M, Normandin MD, Meltzer AC, et al. Pathological correlations of [F-18]-AV-1451 imaging in non-alzheimer tauopathies. Ann Neurol. 2017;81(1):117–128.
11. Kroth H, Oden F, Molette J, et al. Discovery and preclinical characterization of [(18)F]PI-2620, a next-generation tau PET tracer for the assessment of tau pathology in Alzheimer's disease and other tauopathies. Eur J Nucl Med Mol Imaging. 2019;46(10):2178–2189.
12. Rosler TW, Tayaranian Marvian A, Brendel M, et al. Four-repeat tauopathies. Prog Neurobiol. 2019;180:101644.
13. Mormino EC, Toueg TN, Azevedo C, et al. Tau PET imaging with (18)F-PI-2620 in aging and neurodegenerative diseases. Eur J Nucl Med Mol Imaging. 2020;48(7):2233–2244.
14. Brendel M, Barthel H, van Eimeren T, et al. Assessment of 18F-PI-2620 as a biomarker in progressive supranuclear palsy. JAMA Neurol. 2020;77(11):1408–1419.
15. Soleimani-Meigooni DN, Iaccarino L, La Joie R, et al. 18F-flortaucipir PET to autopsy comparisons in Alzheimer's disease and other neurodegenerative diseases. Brain. 2020;143(11):3477–3494.
16. Ghirelli A, Tosakulwong N, Weigand SD, et al. Sensitivity-specificity of tau and amyloid beta positron emission tomography in frontotemporal lobar degeneration. Ann Neurol. 2020;88(5):1009–1022.
17. Lowe VJ, Lundt ES, Albertson SM, et al. Tau-positron emission tomography correlates with neuropathology findings. Alzheimers Dement. 2020;16(3):561–571.
18. Ishizuchi K, Takizawa T, Tezuka T, et al. A case of progressive supranuclear palsy with predominant cerebellar ataxia diagnosed by [(18)F]PM-PBB3 tau PET. J Neurol Sci. 2021;425:117440.
19. Mashima K, Konishi M, Tezuka T, Ito D, Mimura M. A case of tauopathy with auditory agnosia and dysprosody diagnosed by [(18)F]PM-PBB3 tau PET scan. Neurol Sci. 2021;42(8):3471–3474.
20. McKhann GM, Knopman DS, Chertkow H, et al. The diagnosis of dementia due to Alzheimer's disease: Recommendations from the National Institute on Aging-Alzheimer's Association workgroups on diagnostic guidelines for Alzheimer's disease. Alzheimers Dement. 2011;7(3):263–269.
21. Hoglinger GU, Respondek G, Stamelou M, et al. Clinical diagnosis of progressive supranuclear palsy: The movement disorder society criteria. Mov Disord. 2017;32(6):853–864.
22. Armstrong MJ, Litvan I, Lang AE, et al. Criteria for the diagnosis of corticobasal degeneration. Neurology. 2013;80(5):496–503.
23. Rosen WG, Mohs RC, Davis KL. A new rating scale for Alzheimer's disease. Am J Psychiatry. 1984;141(11):1356–1364.
24. Crowe SF. The differential contribution of mental tracking, cognitive flexibility, visual search, and motor speed to performance on parts A and B of the Trail Making Test. J Clin Psychol. 1998;54(5):585–591.
25. Goetz CG, Tilley BC, Shaftman SR, et al. Movement Disorder Society UPDRS Revision Task Force. Movement Disorder Society-sponsored revision of the Unified Parkinson's Disease Rating Scale (MDS-UPDRS): scale presentation and clinimetric testing results. Mov Disord. 2008;23(15):2129–2170.
26. Golbe LI, Ohman-Strickland PA. A clinical rating scale for progressive supranuclear palsy. Brain. 2007;130(6):1552–1565.
27. Iglesias JE, Van Leemput K, Bhatt P, et al. Bayesian segmentation of brainstem structures in MRI. Neuroimage. 2015;113:184–195.
28. Lowe J, Lennox G, Pn L. Disorders of movement and system degeneration, 6th ed. In Greenfield's neuropathology. London, England : Arnold Publisher; 1997.
29. Jellinger K. Progressive supranuclear palsy (subcortical argyrophilic dystrophy). Acta Neuropathol. 1971;19(4):347–352.
30. Arai K, Braak E, de Vos RA, Jansen Steur EN, Braak H. Mossy fiber involvement in progressive supranuclear palsy. Acta Neuropathol. 1999;98(4):341–344.
31. Dickson DW. Neuropathologic differentiation of progressive supranuclear palsy and corticobasal degeneration. J Neurol. 1999;246 (Suppl 2):II6–15.
32. Forman MS, Zhukareva V, Bergeron C, et al. Signature tau neuropathology in gray and white matter of corticobasal degeneration. Am J Pathol. 2002;160(6):2045–2053.
33. Kovacs GG, Lukic MJ, Irwin DJ, et al. Distribution patterns of tau pathology in progressive supranuclear palsy. Acta Neuropathol. 2020;140(2):99–119.
34. Mashima K, Ito D, Kameyama M, et al. Extremely low prevalence of amyloid positron emission tomography positivity in Parkinson's disease without dementia. Eur Neurol. 2017;77(5-6):231–237.
35. Seibyl J, Catafau AM, Barthel H, et al. Impact of training method on the robustness of the visual assessment of 18F-Florbetaben PET scans: Results from a phase-3 study. J Nucl Med. 2016;57(6):900–906.[26823561][Mismatch] 10.2967/jnumed.115.161927
36. Dickson DW, Bergeron C, Chin SS, et al. Office of Rare Diseases neuropathologic criteria for corticobasal degeneration. J Neuropathol Exp Neurol. 2002;61(11):935–946.

37. Lowe VJ, Curran G, Fang P, et al. An autoradiographic evaluation of AV-1451 Tau PET in dementia. Acta Neuropathol Commun. 2016;4(1):58.
38. Ono M, Sahara N, Kumata K, et al. Distinct binding of PET ligands PBB3 and AV-1451 to tau fibril strains in neurodegenerative tauopathies. Brain. 2017;140(3):764–780.
39. Palleis C, Brendel M, Finze A, et al. German Imaging Initiative for Tauopathies (GII4T). Cortical [(18) F]PI-2620 binding differentiates corticobasal syndrome subtypes. Mov Disord. 2021; https://movementdisorders.onlinelibrary.wiley.com/doi/10.1002/mds.28624.
40. Kikuchi A, Okamura N, Hasegawa T, et al. In vivo visualization of tau deposits in corticobasal syndrome by 18F-THK5351 PET. Neurology. 2016;87(22):2309–2316.
41. Brendel M, Schonecker S, Hoglinger G, et al. [(18)F]-THK5351 PET correlates with topology and symptom severity in progressive supranuclear palsy. Front Aging Neurosci. 2017;9:440.
42. Leuzy A, Smith R, Ossenkoppele R, et al. Diagnostic performance of RO948 F 18 tau positron emission tomography in the differentiation of Alzheimer disease from other neurodegenerative disorders. JAMA Neurol. 2020;77(8):955–965.
43. Ishiki A, Harada R, Okamura N, et al. Tau imaging with [(18) F]THK-5351 in progressive supranuclear palsy. Eur J Neurol. 2017; 24(1):130–136.
44. Arima K. Ultrastructural characteristics of tau filaments in tauopathies: Immuno-electron microscopic demonstration of tau filaments in tauopathies. Neuropathology. 2006;26(5):475–483.
45. Arai T, Ikeda K, Akiyama H, et al. Identification of amino-terminally cleaved tau fragments that distinguish progressive supranuclear palsy from corticobasal degeneration. Ann Neurol. 2004; 55(1):72–79.
46. Mueller A, Bullich S, Barret O, et al. Tau PET imaging with (18)F-PI-2620 in patients with Alzheimer disease and healthy controls: A first-in-humans study. J Nucl Med. 2020;61(6):911–919.
47. Marquie M, Verwer EE, Meltzer AC, et al. Lessons learned about [F-18]-AV-1451 off-target binding from an autopsy-confirmed Parkinson's case. Acta Neuropathol Commun. 2017; 5(1):75.
48. Choi JY, Cho H, Ahn SJ, et al. Off-target (18)F-AV-1451 binding in the basal ganglia correlates with age-related iron accumulation. J Nucl Med. 2018;59(1):117–120.
49. Marquie M, Normandin MD, Vanderburg CR, et al. Validating novel tau positron emission tomography tracer [F-18]-AV-1451 (T807) on postmortem brain tissue. Ann Neurol. 2015;78(5):787–800.
50. Aiba I. [Corticobasal syndrome: Recent advances and future directions]. Brain Nerve. 2012;64(4):462–473.
51. Schneider JA, Watts RL, Gearing M, Brewer RP, Mirra SS. Corticobasal degeneration: Neuropathologic and clinical heterogeneity. Neurology. 1997;48(4):959–969.
52. Chiotis K, Saint-Aubert L, Savitcheva I, et al. Imaging in-vivo tau pathology in Alzheimer's disease with THK5317 PET in a multimodal paradigm. Eur J Nucl Med Mol Imaging. 2016;43(9): 1686–1699.